

Determination of the binding and KD probability of the $D_{s0}^*(2317)$ from the $(\bar{D}\bar{K})^-$ mass distributions in $\Lambda_b \rightarrow \Lambda_c(\bar{D}\bar{K})^-$ decays

Hai-Peng Li,¹ Wei-Hong Liang,^{1,2,*} Chu-Wen Xiao,^{1,2,3,†} Ju-Jun Xie,^{4,5,6,‡} and Eulogio Oset^{1,7,§}

¹*Department of Physics, Guangxi Normal University, Guilin 541004, China*

²*Guangxi Key Laboratory of Nuclear Physics and Technology, Guangxi Normal University, Guilin 541004, China*

³*School of Physics, Central South University, Changsha 410083, China*

⁴*Southern Center for Nuclear-Science Theory (SCNT), Institute of Modern Physics, Chinese Academy of Sciences, Huizhou 516000, China*

⁵*Heavy Ion Science and Technology Key Laboratory, Institute of Modern Physics, Chinese Academy of Sciences, Lanzhou 730000, China*

⁶*School of Nuclear Sciences and Technology, University of Chinese Academy of Sciences, Beijing 101408, China*

⁷*Departamento de Física Teórica and IFIC, Centro Mixto Universidad de Valencia-CSIC Institutos de Investigación de Paterna, Apartado 22085, 46071 Valencia, Spain*

We study the $\Lambda_b \rightarrow \Lambda_c \bar{D}^0 K^-$ and $\Lambda_b \rightarrow \Lambda_c D^- \bar{K}^0$ reactions which proceed via a Cabibbo and N_c favored process of external emission, and we determine the $\bar{D}^0 K^-$ and $D^- \bar{K}^0$ mass distributions close to the $\bar{D}\bar{K}$ threshold. For this, we use the tree level contribution plus the rescattering of the meson-meson components, using the extension of the local hidden gauge approach to the charm sector that produces the $D_{s0}^*(2317)$ resonance. We observe a large enhancement of the mass distributions close to threshold due to the presence of this resonance below threshold. Next we undertake the inverse problem of extracting the maximum information on the interaction of the $\bar{D}\bar{K}$ channels from these distributions, and using the resampling method we find that from these data one can obtain precise values of the scattering lengths and effective ranges, the existence of an $I = 0$ bound state with a precision of about 4 MeV in the mass, plus the $\bar{D}\bar{K}$ molecular probability of this state with reasonable precision. Given the fact that the $\Lambda_b \rightarrow \Lambda_c \bar{D}^0 K^-$ reaction is already measured by the LHCb collaboration, it is expected that in the next runs with more statistics of the reaction, these mass distributions can be measured with precision and the method proposed here can be used to determine the nature of the $D_{s0}^*(2317)$, which is still an issue of debate.

I. INTRODUCTION

The $I(J^P) = 0(0^+)$ $D_{s0}^*(2317)$ resonance is a peculiar state. While the quantum numbers allow it to be a standard $c\bar{s}$ state, standard quark models predict P -wave masses much higher than the observed one. The isospin of the state is $I = 0$ according to the PDG [1], but the only observed decay mode is $D_s^+ \pi^0$, which has $I = 1$. This is the mode in which it was first observed [2] and more recent experiments find that the branching ratio to this channel is practically 100% [3]. Due to this isospin violating mode, the width of the state is extremely small. Experimentally it is smaller than 3.8 MeV and theoretical predictions range from 10 keV to 100 keV [4]. Due to the problems of the standard quark model predictions, the molecular picture, as formed from the $D^0 K^+$, $D^+ K^0$, and $D_s^+ \eta$ channels, mostly DK , is most favored [5–12], although other alternatives are also suggested (see review paper on “Heavy Non- $q\bar{q}$ Mesons” [4] in the PDG [1]). Lattice QCD simulations also support this picture [13–16], and in Ref. [17], a detailed analysis of lattice QCD data could quantify the probability of DK in the $D_{s0}^*(2317)$ wave function around 72%. In the molec-

ular picture the state would be bound by about 42 MeV with respect to the $D^0 K^+$ threshold, quite a large binding compared to other claimed molecular states, like the $T_{cc}(3875)$, which are close to some threshold. While the support for this kind of molecular structure is solid from theoretical models [18, 19], it would be good to find experimental data that would support the picture. This would require to involve DK in some reaction, but we know that the state, being bound in this component, cannot decay into this channel. The closest thing we can think of is to investigate experiments in which DK is produced close to threshold and see which information we can obtain from the inspection of the DK invariant mass distributions. Intuitively, we can think that the presence of the DK bound state would produce some enhancement in the DK mass distribution close to threshold. The question is how much, and if one can obtain some information about the $D_{s0}^*(2317)$ from this mass distribution. This is the purpose of the present work. One of such reactions could be $\Lambda_b \rightarrow \Lambda_c \bar{D}^0 K^-$, which has been recently investigated by the LHCb collaboration in Ref. [20]. For the moment, only the ratio of the decay rate to that of the $\Lambda_b^0 \rightarrow \Lambda_c^+ D^-$ reaction, of the order of 20%, has been reported, but future upgrades of LHCb should produce enough statistics to access the mass distribution of $\bar{D}^0 K^-$. With this perspective we prepare the ground to see the potential of this magnitude to learn about the relationship of the $D_{s0}^*(2317)$ state to the DK component.

* liangwh@gxnu.edu.cn

† xiaochw@gxnu.edu.cn

‡ xiejujun@impcas.ac.cn

§ Oset@ific.uv.es

To accomplish this task we do the following work: we study the decays $\Lambda_b \rightarrow \Lambda_c \bar{D}^0 K^-$ and $\Lambda_b \rightarrow \Lambda_c D^- \bar{K}^0$, and evaluate the $\bar{D}^0 K^-$ and $D^- \bar{K}^0$ mass distributions close to their thresholds using the $\bar{D}\bar{K}$ interaction provided by an extension of the local hidden gauge theory [21–24], in which this interaction is driven by the exchange of vector mesons. The only unknown of the theory is a regulator of the loops, which is fitted to get the mass of the $D_{s0}^*(2317)$ state at the experimental mass. Once the theoretical framework is established, we evaluate the mass distributions of $\bar{D}^0 K^-$ and $D^- \bar{K}^0$ close to the threshold, where we observe a large discrepancy with respect to a phase space distribution.

Then comes the second part. We assume that the experiment has been done and mass distributions like those obtained previously are observed. Then we tackle the task of extracting the maximum information about the DK interaction. It is clear that the mass distributions close to the threshold, and far away from the mass of the $D_{s0}^*(2317)$ carry only partial information on the dynamics of the system, but the challenge is to see how much one can learn from it. For this purpose, we assume certain errors, 5% of the value of the differential width, and tackle the inverse problem of determining the interaction from these pseudodata. We make fits to the pseudodata and determine the parameters of the theory. With them we determine the observables, like scattering parameters and the energy of the bound state if it appears. The important thing, however, is the uncertainties in these observables. For this, we use the resampling method [25–27], generating Gaussian weighted distributions of the centroids of the data and carrying a fit for every sample of these pseudodata. Every time the parameters of the interaction are obtained and the observables are evaluated, and after a reasonable number of fits, of the order of 50, we calculate the average of the observables and their dispersion, which provides the uncertainty by which we can determine these observables from these data. The procedure is specially recommended when there are many parameters and one expects correlations between them. We anticipate that we can obtain the scattering lengths and effective ranges with a fair precision, and very important, we also obtain a bound state at the right energy, with an uncertainty in the binding energy of about 4 MeV, much better than the 20 MeV uncertainty that one had in this magnitude for the use of the correlation functions [28]. We can also determine the molecular probability of the DK component of the $D_{s0}^*(2317)$ with an uncertainty of about 11%, also improving the 60% uncertainty obtained for this magnitude from the correlation functions in Ref. [28].

II. FORMALISM AND RESULTS

A. The $D_{s0}^*(2317)$ state in the chiral unitary approach

We have three coupled channels: $\bar{D}^0 K^-$ (1), $D^- \bar{K}^0$ (2), $D_s^- \eta$ (3). The potential for $i \rightarrow j$ transition, using an extension of the local hidden gauge approach [21, 24], is given by

$$V_{ij} = C_{ij} g^2 (p_1 + p_3) \cdot (p_2 + p_4), \quad (1)$$

which projected in S -wave gives

$$V_{ij} = C_{ij} g^2 \frac{1}{2} [3s - (M^2 + m^2 + M'^2 + m'^2) - \frac{1}{s}(M^2 - m^2)(M'^2 - m'^2)], \quad (2)$$

with s the c.m. energy squared, and m, M (m', M') the masses of the light meson and the charmed meson in channel $i(j)$, respectively. The C_{ij} coefficients are given by [28]

$$C_{ij} = \begin{pmatrix} -\frac{1}{2} \left(\frac{1}{M_\rho^2} + \frac{1}{M_\omega^2} \right) & -\frac{1}{M_\rho^2} & \frac{2}{\sqrt{3}} \frac{1}{M_{K^*}^2} \\ & -\frac{1}{2} \left(\frac{1}{M_\rho^2} + \frac{1}{M_\omega^2} \right) & \frac{2}{\sqrt{3}} \frac{1}{M_{K^*}^2} \\ & & 0 \end{pmatrix}, \quad (3)$$

with $M_\rho = 775.2$ MeV, $M_\omega = 775.3$ MeV and $M_{K^*} = 893.6$ MeV.

The $D_{s0}^*(2317)$ bound state is found by searching the pole of the scattering matrix

$$T = [1 - VG]^{-1} V, \quad (4)$$

where $G = \text{diag}(G_i)$, with G_i the loop function of the $\bar{D}\bar{K}$ or $D_s^- \eta$ channel. Following Ref. [28], we have

$$G_i(s) = \int_{|\vec{q}| < q_{\max}} \frac{d^3 q}{(2\pi)^3} \frac{\omega_1 + \omega_2}{2\omega_1 \omega_2} \frac{1}{s - (\omega_1 + \omega_2)^2 + i\epsilon}, \quad (5)$$

with $\omega_1 = \sqrt{M^2 + \vec{q}^2}$, $\omega_2 = \sqrt{m^2 + \vec{q}^2}$ for each of the i channel of the $\bar{D}^0 K^-$, $D^- \bar{K}^0$ and $D_s^- \eta$, and q_{\max} is the regulator of the G function that is a measure of the range of the interaction in momentum space [29, 30].

The T matrix that we obtain and the usual one in Quantum Mechanics have different normalization. Following Ref. [28], we find

$$T = -8\pi \sqrt{s} f^{QM} \approx -8\pi \sqrt{s} \frac{1}{-\frac{1}{a} + \frac{1}{2} r_0 k^2 - ik}, \quad (6)$$

with

$$k = \frac{\lambda^{1/2}(s, m^2, M^2)}{2\sqrt{s}}. \quad (7)$$

TABLE I. Pole position, couplings g_i (in units of MeV) and probabilities P_i , with the cutoff $q_{\max} = 706$ MeV.

pole [MeV]	g_1	g_2	g_3
2317.85	8182.29	8144.59	-5571.38
	P_1	P_2	P_3
	0.34	0.29	0.04

Taking into account that

$$\text{Im} G = -\frac{1}{8\pi\sqrt{s}} k, \quad (8)$$

we find that

$$-\frac{1}{a} + \frac{1}{2} r_0 k^2 \simeq -8\pi\sqrt{s} T^{-1} + ik. \quad (9)$$

Then we can determine the scattering length and effective range for each channel as

$$-\frac{1}{a} = -8\pi\sqrt{s} T^{-1} \Big|_{s=s_{\text{th}}}, \quad (10)$$

$$\begin{aligned} r_0 &= \frac{\partial}{\partial k^2} 2(-8\pi\sqrt{s} T^{-1} + ik) \\ &= \frac{\sqrt{s}}{\mu} \frac{\partial}{\partial s} 2(-8\pi\sqrt{s} T^{-1} + ik) \Big|_{s=s_{\text{th}}}, \end{aligned} \quad (11)$$

where s_{th} is the squared of the energy of the system at threshold ($m + M$) and μ is the reduced mass of m and M .

The couplings are obtained at the pole energy, $\sqrt{s_0}$, considering that

$$T_{ij} \sim \frac{g_i g_j}{s - s_0}, \quad (12)$$

from where

$$g_i^2 = \lim_{s \rightarrow s_0} (s - s_0) T_{11}; \quad g_j = g_1 \lim_{s \rightarrow s_0} \frac{T_{1j}}{T_{11}}, \quad (13)$$

and the probabilities of each channel are obtained as [29, 31, 32]

$$P_i = -g_i^2 \frac{\partial G_i}{\partial s} \Big|_{s=s_0}. \quad (14)$$

With these ingredients, the pole position, couplings g_i of the $D_{s_0}^*(2317)$ state to different channels, and the probabilities P_i are shown in Table I. The scattering lengths a_i and effective ranges $r_{0,i}$ are shown in Table II. Note that the obtained width of the $D_{s_0}^*(2317)$ state is zero, since we did not include its decay channels.

TABLE II. Scattering lengths a_i and effective ranges $r_{0,i}$. [in units of fm]

a_1	a_2	a_3
0.70	$0.51 - i0.12$	$0.21 - i0.06$
$r_{0,1}$	$r_{0,2}$	$r_{0,3}$
-2.25	$0.14 - i2.41$	$0.12 + i0.11$

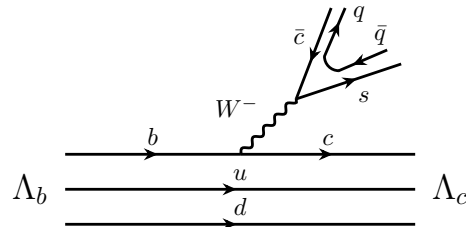


FIG. 1. Decay mechanism for $\Lambda_b \rightarrow \bar{c}s\Lambda_c$ at the quark level. The $\bar{c}s$ component is hadronized inserting $q\bar{q}$ to obtain two mesons.

B. The $K^-\bar{D}^0$, $\bar{K}^0 D^-$ invariant mass distributions for $\Lambda_b \rightarrow \Lambda_c \bar{D}^0 K^-$, $\Lambda_c D^- \bar{K}^0$ decays

In order to evaluate the $\bar{K}\bar{D}$ mass distribution of the $\Lambda_b \rightarrow \Lambda_c^+ \bar{D}^0 K^-$ and $\Lambda_b \rightarrow \Lambda_c^+ D^- \bar{K}^0$, we look at the weak decay process of Fig. 1 at the quark level, which proceeds via a Cabibbo favored process with external emission.

After the $\bar{c}s\Lambda_c$ production, as depicted in Fig. 1, the $\bar{c}s$ pair is hadronized via

$$s\bar{c} \rightarrow \sum_i s\bar{q}_i q_i \bar{c}, \quad q_i = u, d, s, c. \quad (15)$$

This is easily done recalling that $q_i \bar{q}_j$ can be written in terms of physical mesons using the SU(4) matrix of pseudoscalar mesons,

$$\mathcal{P} = \begin{pmatrix} \frac{\eta}{\sqrt{3}} + \frac{\eta'}{\sqrt{6}} + \frac{\pi^0}{\sqrt{2}} & \pi^+ & K^+ & \bar{D}^0 \\ \pi^- & \frac{\eta}{\sqrt{3}} + \frac{\eta'}{\sqrt{6}} - \frac{\pi^0}{\sqrt{2}} & K^0 & D^- \\ K^- & \bar{K}^0 & -\frac{\eta}{\sqrt{3}} + \sqrt{\frac{2}{3}}\eta' & D_s^- \\ D^0 & D^+ & D_s^+ & \eta_c \end{pmatrix}. \quad (16)$$

Forgetting the η' and η_c which do not play a role here, we obtain

$$\begin{aligned} s\bar{c} &\rightarrow \sum_i \mathcal{P}_{3i} \mathcal{P}_{i4} = (\mathcal{P}^2)_{34} \\ &= K^- \bar{D}^0 + \bar{K}^0 D^- - \frac{\eta}{\sqrt{3}} D_s^-. \end{aligned} \quad (17)$$

We can see that we get the $I = 0$ combination of $\bar{K}\bar{D}$, with the isospin multiplets $(\bar{K}^0, -K^-)$, (\bar{D}^0, D^-) , as it should be starting with the $I = 0$ $s\bar{c}$ pair.

In Eq. (17) we see that both $K^-\bar{D}^0$ and $\bar{K}^0 D^-$ are produced at tree level with the same weight. After that

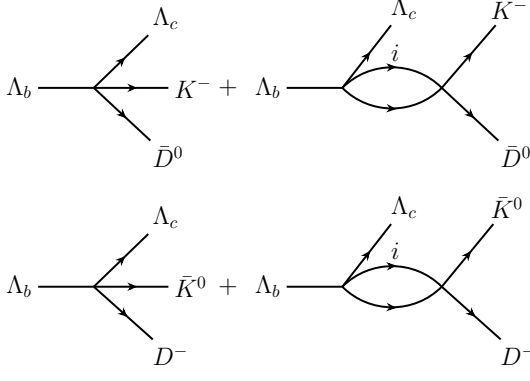


FIG. 2. Diagrams for $\Lambda_b \rightarrow \Lambda_c K^- \bar{D}^0 (\bar{K}^0 D^-)$ with tree level and rescattering mechanisms, with $i = K^- \bar{D}^0, \bar{K}^0 D^-, \eta D_s^-$.

we take into account rescattering of these components, and here the ηD_s^- component also contributes through the $\eta D_s^- \rightarrow \bar{K} \bar{D}$ transition in coupled channels. This is depicted in Fig. 2.

The amplitudes for the two decay processes are then given by

$$t_{K^- \bar{D}^0} = A \left\{ 1 + G_{K^- \bar{D}^0} t_{K^- \bar{D}^0, K^- \bar{D}^0} + G_{\bar{K}^0 D^-} t_{\bar{K}^0 D^-, K^- \bar{D}^0} - \frac{1}{\sqrt{3}} G_{\eta D_s^-} t_{\eta D_s^-, K^- \bar{D}^0} \right\}, \quad (18)$$

$$t_{\bar{K}^0 D^-} = A \left\{ 1 + G_{K^- \bar{D}^0} t_{K^- \bar{D}^0, \bar{K}^0 D^-} + G_{\bar{K}^0 D^-} t_{\bar{K}^0 D^-, \bar{K}^0 D^-} - \frac{1}{\sqrt{3}} G_{\eta D_s^-} t_{\eta D_s^-, \bar{K}^0 D^-} \right\}, \quad (19)$$

where A is an arbitrary constant.

The partial decay width reads

$$\frac{d\Gamma}{dM_{\text{inv}}} = \frac{1}{(2\pi)^3} \frac{1}{4M_{\Lambda_b}^2} p_{\Lambda_c} \tilde{p}_{\bar{K}} \sum \sum |t|^2, \quad (20)$$

with

$$p_{\Lambda_c} = \frac{\lambda^{1/2}(M_{\Lambda_b}^2, M_{\Lambda_c}^2, M_{\text{inv}}^2(\bar{K}\bar{D}))}{2M_{\Lambda_b}}, \quad (21)$$

$$\tilde{p}_{\bar{K}} = \frac{\lambda^{1/2}(M_{\text{inv}}^2(\bar{K}\bar{D}), M_{\bar{K}}^2, M_{\bar{D}}^2)}{2M_{\text{inv}}(\bar{K}\bar{D})}. \quad (22)$$

The obtained $K^- \bar{D}^0$ and $\bar{K}^0 D^-$ invariant mass distributions are shown in Fig. 3, taking $A = 1$. We can see that compared to phase space, with a constant t and normalized to the same area below the curves, the $K^- \bar{D}^0$ and $\bar{K}^0 D^-$ mass distributions have an important enhancement close to threshold, which is due to the presence of the $D_{s0}^*(2317)$ resonance below threshold. The peak observed in the $\bar{D}^0 K^-$ mass distribution is due to the opening of the $D^- \bar{K}^0$ channel.

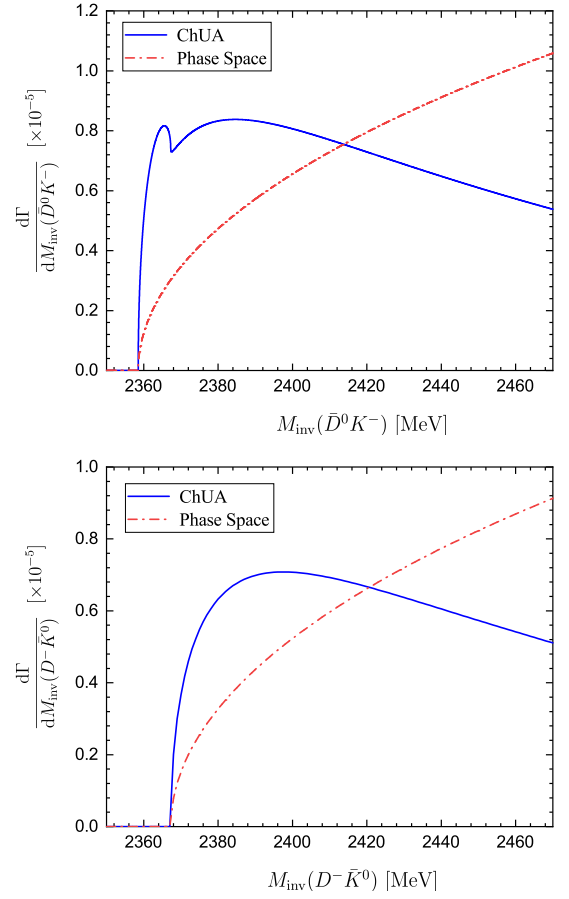


FIG. 3. The invariant mass distributions of $\bar{D}^0 K^-$ (up) and $D^- \bar{K}^0$ (down) using the local hidden gauge approach.

It is thus clear that these invariant mass distributions bear information on the existence of a bound state below threshold. The question is if we can determine the binding of this state, and with which precision, from these distributions. This problem is tackled in the next subsection.

C. Inverse problem

In order to obtain the properties of the bound state and the scattering magnitudes, we follow a minimum model dependent approach and take the potential matrix, as done in Ref. [28],

$$V = \begin{pmatrix} V_{11} & V_{12} & V_{13} \\ & V_{11} & V_{13} \\ & & 0 \end{pmatrix}, \quad (23)$$

with

$$V_{11} = V'_{11} + \frac{\alpha}{M_V^2} (s - \bar{s}), \quad (24)$$

$$V_{12} = V'_{12} + \frac{\beta}{M_V^2}(s - \bar{s}), \quad (25)$$

$$V_{13} = V'_{13} + \frac{\gamma}{M_V^2}(s - \bar{s}), \quad (26)$$

where \bar{s} is the energy squared of the $\bar{D}^0 K^-$ threshold, and the factor M_V^2 is introduced to make the parameters α , β and γ dimensionless. Eq. (23) implicitly assumes that the potential V is isospin symmetric (isospin can be a bit broken with the unitarization, due to different masses in the same isospin multiplets). This implies that in the general V_{ij} ($i = 1, 2, 3$) matrix, $V_{11} = V_{22}$ and $V_{13} = V_{23}$ [28]. On the other hand, the energy dependence introduced in Eqs. (24)-(26) is done to take into account the possible contributions of other channels, as for instance components of a genuine state [30, 33].

The strategy now is to start from the two mass distributions, carry a fit to the curves, determine the free parameters of the theory and use them to evaluate the observables. For this purpose, we take as pseudodata the values obtained with the local hidden gauge approach. We take 30 points equally spaced in energy and assume an “experimental error” of 5% of the value. The error of the values and one example of the Gaussian randomly generated values from the resampling are shown in Fig. 4.

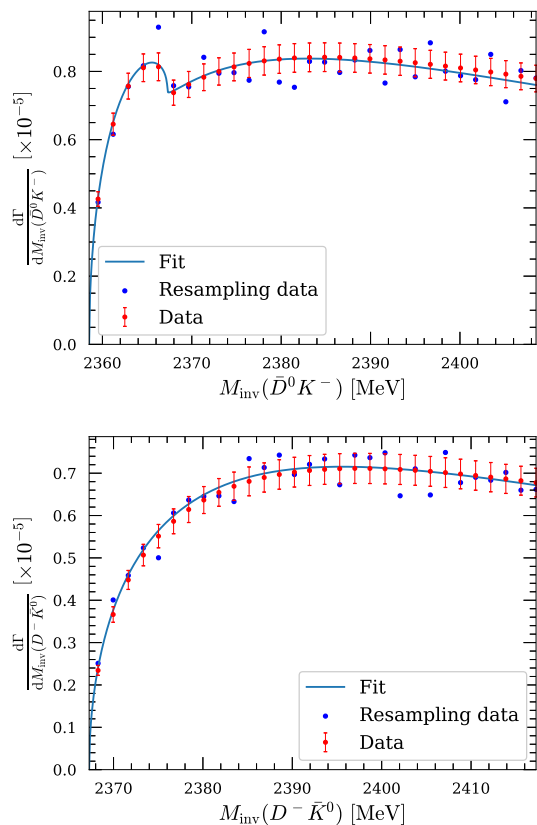


FIG. 4. Pseudodata taken from the local hidden gauge approach of Subsection III A. The scattered points are one example of a Gaussian randomly generated centroids of the data that simulates an actual experimental measurement.

As mentioned in the Introduction, we use the resampling method. We have V'_{11} , V'_{12} , V'_{13} , α , β , γ , q_{\max} and A as free parameters. It looks like quite many parameters, not completely independent, meaning that there could be correlations between them and different sets of parameters could lead to the same solution. This is actually the case and this is where the resampling method gets its strength. In each of the fits of the resampling, the fit parameters could be different, but what matters is the values obtained for the observables. We take the average of each of them and their dispersion, and the results are shown in Table III for the parameters, in Table IV for the pole position and the couplings g_i , in Table V for scattering lengths a_i and effective ranges $r_{0,i}$, and in Table VI for the probabilities P_i .

Since the isospin states of $\bar{K}\bar{D}$ are given by

$$|\bar{K}\bar{D}, I = 0\rangle = \frac{1}{\sqrt{2}} |\bar{K}^0 D^- + K^- \bar{D}^0\rangle, \quad (27)$$

$$|\bar{K}\bar{D}, I = 1\rangle = \frac{1}{\sqrt{2}} |\bar{K}^0 D^- - K^- \bar{D}^0\rangle, \quad (28)$$

the potentials for isospin $I = 0$, $I = 1$ are given by

$$V^{I=0} = \frac{1}{2}(V_{11} + V_{22} + 2V_{12}) = V_{11} + V_{12}, \quad (29)$$

$$V^{I=1} = \frac{1}{2}(V_{11} + V_{22} - 2V_{12}) = V_{11} - V_{12}. \quad (30)$$

We can see that with the results of Table III, the $I = 0$ interaction is attractive, leading to the $D_{s0}^*(2317)$ state, while the interaction in $I = 1$ is repulsive and we get no state there. The state that we get corresponds to $I = 0$. We can also conclude this from inspection of the couplings, g_1 , g_2 which are practically identical, indicating according to Eq. (27) that we have an $I = 0$ state.

We observe that the uncertainties in the parameters are not small, particularly for α , β , γ . This is a reflection of the existence of correlations between the parameters, but, as mentioned, what matters is not the values of the parameters but those of the observables and those are obtained with relatively high precision. Indeed a_1 for $\bar{D}^0 K^-$ is real and has an uncertainty of 14%, a_2 for $D^- \bar{K}^0$ is complex (the $\bar{D}^0 K^-$ channel is open for decay) and has uncertainties of about 17% and 27% in the real and imaginary parts respectively. On the other hand, the ηD_s^- channel, which is far away from the $\bar{K}\bar{D}$ thresholds, is also determined but with uncertainties of about 50% and 40% in the real and imaginary parts, respectively. The effective ranges $r_{0,1}$, $r_{0,2}$ are determined with much bigger uncertainties and $r_{0,3}$ cannot be determined, since the uncertainties are much bigger than the central values. Very interesting is the results obtained for the pole position, which appear with the right mass and an uncertainty of about 4 MeV, quite remarkable knowing that the state is bound by 42 MeV. The data around the $\bar{K}\bar{D}$ threshold allowed us to find a pole 42 MeV below it. As shown in Table VI, the probabilities are obtained with about 16% accuracy, with 11% errors in the

TABLE III. Values of parameters by fitting the resampled data from thresholds up to 50 MeV above thresholds.

V'_{11}	V'_{12}	V'_{13}	α
-89.71 ± 31.50	-130.48 ± 27.73	98.15 ± 10.03	38.41 ± 128.72
β	γ	q_{\max} [MeV]	A
-103.88 ± 120.34	7.28 ± 33.75	688.38 ± 32.87	0.95 ± 0.09

TABLE IV. The average and dispersion for pole position and couplings. [in units of MeV]

pole	g_1	g_2	g_3
2319.32 ± 3.92	8480.92 ± 612.18	8436.40 ± 578.85	-6594.20 ± 927.89

TABLE V. Average value and dispersion of scattering length a_i and effective range $r_{0,i}$ for channel i . [in units of fm]

a_1	a_2	a_3
0.77 ± 0.11	$(0.59 \pm 0.10) - i(0.11 \pm 0.03)$	$(0.18 \pm 0.09) - i(0.05 \pm 0.02)$
$r_{0,1}$	$r_{0,2}$	$r_{0,3}$
-1.80 ± 0.64	$(0.42 \pm 1.09) - i(1.49 \pm 0.77)$	$-(2.75 \pm 4.33) - i(1.00 \pm 1.72)$

TABLE VI. The average and dispersion for the probability.

P_1	P_2	P_3
0.38 ± 0.06	0.32 ± 0.05	0.05 ± 0.01

sum of $P_1 + P_2$ summing relative errors in quadrature. The individual probabilities are $P_1 = 0.38$ for $\bar{D}^0 K^-$ and $P_2 = 0.32$ for $D^- \bar{K}^0$. $P_1 + P_2 \approx 0.7$ indicating that we have largely a bound state of $\bar{K} \bar{D}$.

In Fig. 5 we also show the results of the resampling with a narrow band for the uncertainty. Altogether we see that we could extract a large amount of information from the analysis of the $\bar{D}^0 K^-$ and $D^- \bar{K}^0$ invariant mass distributions close to threshold from the $\Lambda_b \rightarrow \Lambda_c \bar{D}^0 K^-$ and $\Lambda_b \rightarrow \Lambda_c D^- \bar{K}^0$ decays.

III. CONCLUSIONS

We have studied the $\Lambda_b \rightarrow \Lambda_c \bar{D}^0 K^-$ and $\Lambda_b \rightarrow \Lambda_c D^- \bar{K}^0$ reactions and shown that they proceed via a weak decay mechanism of external emission which is Cabibbo and N_c favored. After the quark level decay is identified, we proceed to hadronize the produced $s\bar{c}$ pair into two mesons and find that $\bar{D}^0 K^-$ and $D^- \bar{K}^0$ are produced with equal weight, together with ηD_s^- . The next step consist in allowing these components to undergo final state interaction (rescattering) to finally have the desired final state. The interaction of the $\bar{D}^0 K^-$, $D^- \bar{K}^0$ and ηD_s^- channels is constructed using an extension of the local hidden gauge approach that gives rise to the $D_{s0}^*(2317)$ state. The rescattering procedure leads to

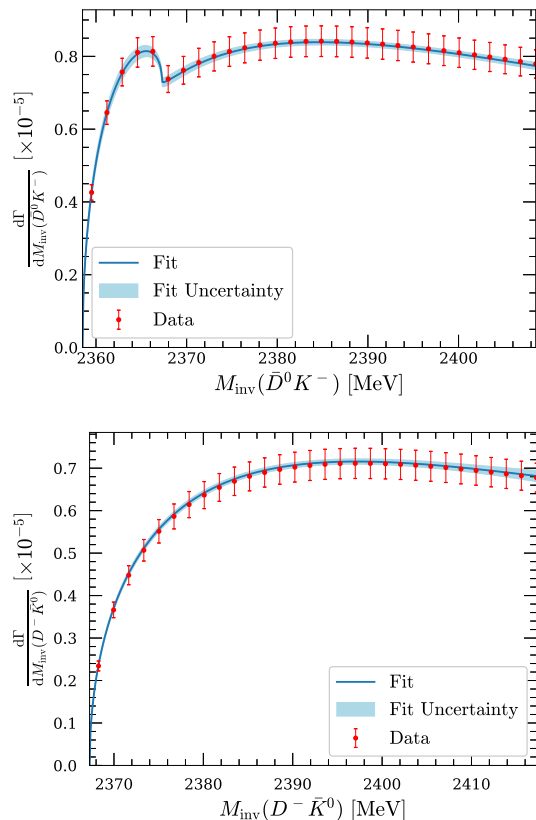


FIG. 5. Results of the fit from the resampling procedure with the error band (see the text).

$\bar{D}^0 K^-$ and $D^- \bar{K}^0$ mass distributions, peaking sharply at threshold, that differ appreciably from phase space.

This is due to the presence of the $D_{s_0}^*(2317)$ resonance which is bound by 42 MeV but makes itself be felt at the threshold of the $\bar{D}\bar{K}$.

The next step consist in assuming that the $\bar{D}^0 K^-$ and $D^- \bar{K}^0$ mass distributions are measured in a certain span of invariant masses (so far only branching ratios are measured for the first reaction), and we try to see what information can be obtained from them using a minimum model dependent method to analyze the data. For this purpose, we assume that the data are those given by the local hidden gauge approach and carry a fit to these data. We use then a general transition potential between the channels, with the matrix elements of the potential considered as free parameters. We make these matrix elements energy dependent to take into account possible missing channels or the existence of a genuine state of nonmolecular nature, such that, should the $D_{s_0}^*(2317)$ state not be a molecular state, the fit could take that into account. We should note that in the case that the $D_{s_0}^*(2317)$ state was not linked to the $\bar{D}\bar{K}$ components we should not expect any enhancement in the $\bar{D}^0 K^-$ and $D^- \bar{K}^0$ mass distributions at threshold due to the presence of that state. Hence, the data will tell us if this is the case or not. For the moment we assumed that the data are those of the local hidden gauge approach that generates the $D_{s_0}^*(2317)$ state and we carry a fit to the data.

The procedure of the fit is done using the resampling method, specially advised when there are correlations between the parameters of the theory, as we have in the present case. We generate randomly gaussian points of the mass distributions and carry a fit to these pseudodata many times obtaining the parameters of the theory, and then we evaluate the scattering lengths and effective ranges plus the pole position (if a pole appears which is the case) for each resampled set of pseudodata. Finally the average of all these observables and their dispersion are evaluated. We find that these data allow us to obtain good values of the scattering lengths with small un-

certainties, and also values for the effective ranges with larger uncertainties. The most remarkable fact is that we can obtain a pole corresponding to a state of $I = 0$ at the right position of the $D_{s_0}^*(2317)$ and with uncertainty of only 4 MeV in the mass, assuming about 5% error in the strength of the mass distributions. We are also able to determine the molecular probability of the $\bar{D}\bar{K}$ component with an uncertainty of about 11%. These results are telling us the great potential that these data have in order to determine scattering parameters of the $\bar{D}^0 K^-$ and $D^- \bar{K}^0$ pairs and the molecular nature of the $D_{s_0}^*(2317)$. In view of these excellent results, we can only encourage the measurement of these mass distributions, only one step forward from present measurements on these reactions at LHCb, that could be accomplished in the next planned run in the CERN facility.

ACKNOWLEDGMENTS

We would like to acknowledge first results from Natsumi Ikeno showing the mass distributions of $\bar{K}^0 D^-$ and $K^- \bar{D}^0$ at threshold, as reported in this paper. This work is partly supported by the National Natural Science Foundation of China (NSFC) under Grants No. 12365019, No. 11975083, No. 12075288, No. 12435007, and No. 12361141819, and by the Central Government Guidance Funds for Local Scientific and Technological Development, China (No. Guike ZY22096024), and by the Natural Science Foundation of Guangxi province under Grant No. 2023JJA110076, and partly by the Natural Science Foundation of Changsha under Grant No. kq2208257 and the Natural Science Foundation of Hunan province under Grant No. 2023JJ30647 (CWX). This work is supported partly by the Spanish Ministerio de Ciencia e Innovación (MICINN) under contracts PID2020-112777GB-I00, PID2023-147458NB-C21 and CEX2023-001292-S; by Generalitat Valenciana under contracts PROMETEO/2020/023 and CIPROM/2023/59.

-
- [1] S. Navas *et al.* (Particle Data Group), Review of particle physics, *Phys. Rev. D* **110**, 030001 (2024).
 - [2] B. Aubert *et al.* (BaBar), Observation of a narrow meson decaying to $D_s^+ \pi^0$ at a mass of 2.32-GeV/ c^2 , *Phys. Rev. Lett.* **90**, 242001 (2003), [arXiv:hep-ex/0304021](#).
 - [3] M. Ablikim *et al.* (BESIII), Measurement of the absolute branching fraction of $D_{s_0}^{*\pm}(2317) \rightarrow \pi^0 D_s^\pm$, *Phys. Rev. D* **97**, 051103 (2018), [arXiv:1711.08293 \[hep-ex\]](#).
 - [4] T. Gutsche, C. Hanhart, and R. Mitchell, Heavy Non- $q\bar{q}$ Mesons, review paper in the PDG [1].
 - [5] E. van Beveren and G. Rupp, Observed $D_s(2317)$ and tentative $D(2100-2300)$ as the charmed cousins of the light scalar nonet, *Phys. Rev. Lett.* **91**, 012003 (2003), [arXiv:hep-ph/0305035](#).
 - [6] T. Barnes, F. E. Close, and H. J. Lipkin, Implications of a DK molecule at 2.32-GeV, *Phys. Rev. D* **68**, 054006 (2003), [arXiv:hep-ph/0305025](#).
 - [7] Y.-Q. Chen and X.-Q. Li, A Comprehensive four-quark interpretation of $D_{(s)}(2317)$, $D_{(s)}(2457)$ and $D_{(s)}(2632)$, *Phys. Rev. Lett.* **93**, 232001 (2004), [arXiv:hep-ph/0407062](#).
 - [8] E. E. Kolomeitsev and M. F. M. Lutz, On Heavy light meson resonances and chiral symmetry, *Phys. Lett. B* **582**, 39 (2004), [arXiv:hep-ph/0307133](#).
 - [9] D. Gamermann, E. Oset, D. Strottman, and M. J. Vicente Vacas, Dynamically generated open and hidden charm meson systems, *Phys. Rev. D* **76**, 074016 (2007), [arXiv:hep-ph/0612179](#).
 - [10] F.-K. Guo, P.-N. Shen, and H.-C. Chiang, Dynamically generated 1^+ heavy mesons, *Phys. Lett. B* **647**, 133 (2007), [arXiv:hep-ph/0610008](#).
 - [11] Z. Yang, G.-J. Wang, J.-J. Wu, M. Oka, and S.-L. Zhu, Novel Coupled Channel Framework Connecting the Quark Model and Lattice QCD for the Near-

- threshold D_s States, *Phys. Rev. Lett.* **128**, 112001 (2022), [arXiv:2107.04860 \[hep-ph\]](#).
- [12] M.-Z. Liu, X.-Z. Ling, L.-S. Geng, En-Wang, and J.-J. Xie, Production of $D_{s0}^*(2317)$ and $D_{s1}(2460)$ in B decays as $D^{(*)}K$ and $D_s^{(*)}\eta$ molecules, *Phys. Rev. D* **106**, 114011 (2022), [arXiv:2209.01103 \[hep-ph\]](#).
- [13] D. Mohler, C. B. Lang, L. Leskovec, S. Prelovsek, and R. M. Woloshyn, $D_{s0}^*(2317)$ Meson and D -Meson-Kaon Scattering from Lattice QCD, *Phys. Rev. Lett.* **111**, 222001 (2013), [arXiv:1308.3175 \[hep-lat\]](#).
- [14] C. B. Lang, L. Leskovec, D. Mohler, S. Prelovsek, and R. M. Woloshyn, D_s mesons with DK and D^*K scattering near threshold, *Phys. Rev. D* **90**, 034510 (2014), [arXiv:1403.8103 \[hep-lat\]](#).
- [15] G. S. Bali, S. Collins, A. Cox, and A. Schäfer, Masses and decay constants of the $D_{s0}^*(2317)$ and $D_{s1}(2460)$ from $N_f = 2$ lattice QCD close to the physical point, *Phys. Rev. D* **96**, 074501 (2017), [arXiv:1706.01247 \[hep-lat\]](#).
- [16] G. K. C. Cheung, C. E. Thomas, D. J. Wilson, G. Moir, M. Peardon, and S. M. Ryan (Hadron Spectrum), DK $I = 0, D\bar{K}$ $I = 0, 1$ scattering and the $D_{s0}^*(2317)$ from lattice QCD, *JHEP* **02**, 100, [arXiv:2008.06432 \[hep-lat\]](#).
- [17] A. Martínez Torres, E. Oset, S. Prelovsek, and A. Ramos, Reanalysis of lattice QCD spectra leading to the $D_{s0}^*(2317)$ and $D_{s1}^*(2460)$, *JHEP* **05**, 153, [arXiv:1412.1706 \[hep-lat\]](#).
- [18] J.-J. Xie and E. Oset, Role of the $f_1(1285)$ state in the $J/\psi \rightarrow \phi\bar{K}K^*$ and $J/\psi \rightarrow \phi f_1(1285)$ decays, *Phys. Lett. B* **753**, 591 (2016), [arXiv:1509.08099 \[hep-ph\]](#).
- [19] J.-X. Lin, J.-T. Li, W.-H. Liang, H.-X. Chen, and E. Oset, J/ψ decays into $\omega(\phi)f_1(1285)$ and $\omega(\phi)“f_1(1420)”$, *Eur. Phys. J. C* **84**, 52 (2024), [arXiv:2310.19213 \[hep-ph\]](#).
- [20] R. Aaij *et al.* (LHCb), Observation of $\Lambda_b^0 \rightarrow \Lambda_c^+ \bar{D}^{(*)0} K^-$ and $\Lambda_b^0 \rightarrow \Lambda_c^+ D_s^{*-} K^-$ decays, *Eur. Phys. J. C* **84**, 575 (2024), [arXiv:2311.14088 \[hep-ex\]](#).
- [21] M. Bando, T. Kugo, and K. Yamawaki, Nonlinear Realization and Hidden Local Symmetries, *Phys. Rept.* **164**, 217 (1988).
- [22] M. Harada and K. Yamawaki, Hidden local symmetry at loop: A New perspective of composite gauge boson and chiral phase transition, *Phys. Rept.* **381**, 1 (2003), [arXiv:hep-ph/0302103](#).
- [23] U. G. Meissner, Low-Energy Hadron Physics from Effective Chiral Lagrangians with Vector Mesons, *Phys. Rept.* **161**, 213 (1988).
- [24] H. Nagahiro, L. Roca, A. Hosaka, and E. Oset, Hidden gauge formalism for the radiative decays of axial-vector mesons, *Phys. Rev. D* **79**, 014015 (2009), [arXiv:0809.0943 \[hep-ph\]](#).
- [25] W. Press, S. Teukolsky, W. Vetterling, and B. Flannery, Numerical recipes in FORTRAN: The art of scientific computing (1992).
- [26] B. Efron and R. Tibshirani, An introduction to the bootstrap, *Statist. Sci.* **57**, 54 (1986).
- [27] M. Albaladejo, D. Jido, J. Nieves, and E. Oset, $D_{s0}^*(2317)$ and DK scattering in B decays from BaBar and LHCb data, *Eur. Phys. J. C* **76**, 300 (2016), [arXiv:1604.01193 \[hep-ph\]](#).
- [28] N. Ikeno, G. Toledo, and E. Oset, Model independent analysis of femtoscopic correlation functions: An application to the $D_{s0}^*(2317)$, *Phys. Lett. B* **847**, 138281 (2023), [arXiv:2305.16431 \[hep-ph\]](#).
- [29] D. Gamermann, J. Nieves, E. Oset, and E. Ruiz Arriola, Couplings in coupled channels versus wave functions: application to the $X(3872)$ resonance, *Phys. Rev. D* **81**, 014029 (2010), [arXiv:0911.4407 \[hep-ph\]](#).
- [30] J. Song, L. R. Dai, and E. Oset, How much is the compositeness of a bound state constrained by a and r_0 ? The role of the interaction range, *Eur. Phys. J. A* **58**, 133 (2022), [arXiv:2201.04414 \[hep-ph\]](#).
- [31] T. Hyodo, Structure and compositeness of hadron resonances, *Int. J. Mod. Phys. A* **28**, 1330045 (2013), [arXiv:1310.1176 \[hep-ph\]](#).
- [32] T. Hyodo, D. Jido, and A. Hosaka, Compositeness of dynamically generated states in a chiral unitary approach, *Phys. Rev. C* **85**, 015201 (2012), [arXiv:1108.5524 \[nucl-th\]](#).
- [33] F. Aceti, L. R. Dai, L. S. Geng, E. Oset, and Y. Zhang, Meson-baryon components in the states of the baryon decuplet, *Eur. Phys. J. A* **50**, 57 (2014), [arXiv:1301.2554 \[hep-ph\]](#).